HAL
open science

Sol-Gel Routes to Replace Chromate Based Treatments for Protection Against Zinc Corrosion

Vincent Meiffren, Pascal Lenormand, Florence Ansart, Stéphan Manov

To cite this version:

Vincent Meiffren, Pascal Lenormand, Florence Ansart, Stéphan Manov. Sol-Gel Routes to Replace Chromate Based Treatments for Protection Against Zinc Corrosion. ECS Transactions, 2011, 35 (17), pp.75-87. 10.1149/1.3641292 . hal-02475643

HAL Id: hal-02475643

https://hal.science/hal-02475643v1

Submitted on 12 Feb 2020

HAL is a multi-disciplinary open access archive for the deposit and dissemination of scientific research documents, whether they are published or not. The documents may come from teaching and research institutions in France or abroad, or from public or private research centers.

L'archive ouverte pluridisciplinaire **HAL**, est destinée au dépôt et à la diffusion de documents scientifiques de niveau recherche, publiés ou non, émanant des établissements d'enseignement et de recherche français ou étrangers, des laboratoires publics ou privés.

Open Archive Toulouse Archive Ouverte (OATAO)

OATAO is an open access repository that collects the work of Toulouse researchers and makes it freely available over the web where possible

This is an author's version published in: http://oatao.univ-toulouse.fr/24431

Official URL: https://doi.org/10.1149/1.3641292

To cite this version:

Meiffren, Vincent and Lenormand, Pascal and Ansart, Florence and Manov, Stéphan *Sol-Gel Routes to Replace Chromate Based Treatments for Protection Against Zinc Corrosion.* (2011) ECS Transactions, 35 (17). 75-87. ISSN 1938-5862

Any correspondence concerning this service should be sent to the repository administrator: tech-oatao@listes-diff.inp-toulouse.fr

10.1149/1.3641292

Sol-gel routes to replace chromate based treatments for protection against zinc corrosion

V. Meiffren[a], P. Lenormand[a], F. Ansart[a], S. Manov[a]

[a] CIRIMAT - LCMIE, 118 route de Narbonne, 31042 Toulouse cedex 9, France

Regarding the environmental consciousness and requirements relative to industrial processes, researchers and end users have to move to more green surface treatments. That is why, the use of toxic compounds such as chromates must be strictly prohibited. So, in order to replace this element preserving an efficient protection against corrosion of metals, a new route using sol-gel process clearly appears as a promising alternative method.
In this paper, we investigated three different sol-gel systems in various media (alcohol and/or water) and compared their efficiency in terms of protection against corrosion and environmentally friendliness. Thus, industrial normalized corrosion test and electrochemical analyses such as polarisation curves and EIS measurements were carried out in order to both evaluate and discuss coatings behaviour in corrosive environment.

Introduction

Protection against corrosion is well known as one of the most important issue in many fields. Regarding metals, the improvement of the protection leads to an increase of the lifetime and allows metal using in more applications. Relative to zinc metal, anticorrosive treatments are needed to slow down oxidation of the surface when pollutants, present in the atmosphere react with the metal. In fact, under chloride or sulfur exposure, zinc reacts by forming white rust (1). Instead of the metal degradation, the visual aspect is strongly damaged, which is a main drawback in the building field. Usually, zinc protection was obtained by forming conversion coatings on the metal, and like many other metals, chromates were the most efficient corrosion inhibitor (2). But, nowadays, industrial processes have to turn to more “green” routes and chromate compounds will be strictly forbidden in the next years.
So, in this study, our goal is to propose alternative routes to protect zinc avoiding the use of toxic elements as chromates. Therefore, the amount of VOC contained in the solutions has to be studied. In order to reach both objectives: good performances and environmental aspects, sol-gel route has been chosen in association with dip-coating process because no toxic compounds are used, it is easy-to-use, low cost process and layers can form efficient physical barriers (3-11).
Based on our previous works (12-14), three different coatings have been studied to define the best compromise between protection efficiency and environmentally friendliness. The first one was made from TEOS (tetraethoxysilane) and MAP (γ-methacryloxypropyl trimethoxysilane) which leads to very high protection against corrosion (12) but with a too high amount of alcohol. And two other processes correspond to very low alcohol content in the solution or alcohol free solution, respectively called:

1) GPTMS (3-glycidoxypropyltrimethoxysilane) and ASB (Aluminum-tri-sec butoxide) (14).
2) Bisamino (Bis [3-(trimethoxysilyl)-propyl] amine) (13).

Developed formulas of these precursors are indicated in the figure 1.

TEOS	MAP	ASB
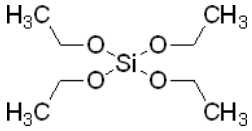	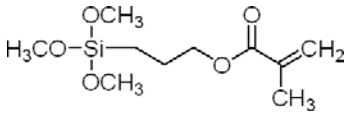	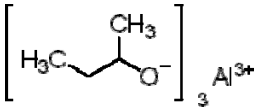

GPTMS	Bisamino
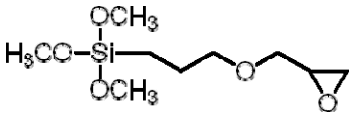	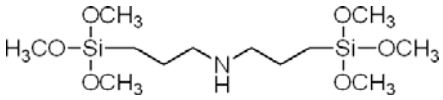

Figure 1. Developed formulas of precursors

To characterize the protective properties, accelerated corrosion tests coupled with electrochemical analyses were carried out. More precisely, thickness influence on barrier properties and coatings behavior during long term immersion was investigated in order to understand the degradation mechanisms.

Material and methods

Pre-treatment of the substrate

Rolled and mechanically brushed zinc strip (0.7mm thick) was used as substrate. Samples (25x80mm) were cut and cleaned with ethanol, and then immersed in a commercial alkaline solution (Novaclean®) during 5 min at 80°C in order to remove the top oxide layer and to improve the wettability. By this way, the cleaned zinc has an average roughness (Ra) of 0.6µm.

Preparation of sols

Generally, sol-gel precursors for low temperature applications are metallic alkoxides MOR_n type, with more often silicon atom as metal. However, many studies have shown good anticorrosive properties using hybrid layers obtained by adding an organic part to the network (6,11,15-17). Therefore, precursors containing an organic group linked to the metal are frequently used such as (R'_mMOR_n) (5).

Relative to the sol preparation, it consists of mixing precursor(s) with solvent(s) (water and/or alcohol). Two series of reactions started between water and precursor (hydrolysis [1]) and then with the hydrolyzed precursor and another precursor, hydrolyzed or not (homo and hetero-condensation respectively [2] and [3]) to form M-O-M bonds. These bonds are then the elementary units of the future inorganic network obtained after the drying step.

Hydrolysis:

$$\equiv M{-}OR + H_2O \rightarrow \equiv M{-}OH + R{-}OH \quad [1]$$

Condensation:

$$\equiv M{-}OH + \equiv M{-}OH \rightarrow \equiv M{-}O{-}M \equiv + H_2O \quad [2]$$

or

$$\equiv M{-}OH + \equiv M{-}OR \rightarrow \equiv M{-}O{-}M \equiv + R{-}OH \quad [3]$$

In this study, three sols consisting of different precursors have been prepared:
Sol A: TEOS (tetraethoxy silane) and MAP (γ-methacryloxypropyl trimethoxysilane) were mixed in a molecular ratio of 8/1 with [TEOS]=1mol/L, then added to the solvent, ethanol and water in molecular ratio of 1.3/1. Hydrolysis rate ([H_2O]/[precursors] was fixed at 7/1.
Sol B: GPTMS (3-glycidoxypropyltrimethoxysilane) and ASB (Aluminum-tri-sec butoxide) mixed to propan-2-ol are vigorously stirred in molar ratio of 7/3/3. Afterwards, water is added to the solution with a hydrolysis rate of 13.8.
Sol C: Bisamino (Bis [3-(trimethoxysilyl)-propyl] amine) is added to acidified water with [Bisamino]=[HNO_3] and a hydrolysis rate of 163.

In all sols, 0.01mol/L of cerium nitrate has been introduced with the aqueous phase because of this concentration corresponds to the best compromise for the corrosion inhibitive properties (18,19).

Hybrid coatings processing

Before deposition, sols A and B were aged during 24h and only during 10min for the sol C, depending on the hydrolysis rate and so the reactions kinetics. Coatings were then performed by dip-coating process using a controlled withdrawal rate of 20cm/min followed by different thermal treatments. For coating A (obtained from the sol A), samples were dried at 60°C during 15min. For the coatings B, drying conditions were 20h at 50°C followed by 16h at 110°C. And for the coatings C, thermal treatment corresponded to 72h at 80°C.

Characterisation techniques

Microstructure of sol-gel coatings has been studied using scanning electronic microscopy (surfaces and cross sections).

In parallel, corrosion resistance of coated zinc was evaluated through a cyclic corrosion test which is a more conventional industrial test. Test duration was 10 cycles, 24h each. One cycle consists in different steps alternating wet and dry atmospheres at different temperatures. During the humidity stage, the chamber was maintained at near 100% relative humidity. In order to estimate the white rust formation, the samples were weighted before and after all corrosion cycles.

Anticorrosion properties were also evaluated thanks to electrochemical measurements. On the first hand, polarization curves have been performed in aerated and unstirred 0.5mol/L of NaCl aqueous solution. Saturated calomel electrode, connected to the working solution through a capillary, was used as reference, and a Pt electrode as auxiliary electrode. 1 cm² of the working electrode was exposed to the corrosive solution. Polarization curves were plotted using a PGP 201 Potentiostat/Galvanostat device. Polarization curves were recorded for all samples in a potential range from free open circuit potential to -0.850V, in order to study the anodic behavior of treated zinc. On the

second hand, EIS measurements were carried out on 5 cm2 covered area in a 0.5mol/L Na_2SO_4 electrolyte. Spectra were recorded over a frequency range between 65kHz and 100mHz with an amplitude of 10mV. Both Bode and Nyquist plots were used to determine sample behavior. All electrochemical measurements were performed after stabilization of the potential during 1h.

Results and discussion

Correlation between sols characteristics and coating microstructure

Sols are limpid and homogenous excepted for sol C where some particles appeared when water was mixed to the precursor. This formation is probably due to the high hydrolysis rate. Alcohol is generally added to the solution to reduce the hydrolysis kinetics but, Bisamino compound hydrolysis is extremely quick.

Sol viscosities were quite similar, between 2mPa.s and 3mPa.s respectively for the sol TEOS/MAP and sol Bisamino, and around 9mPa.s for sol GPTMS/ASB. Viscosity differences are only due to precursor concentrations. After deposition by dip-coating and drying as described before, samples were weighted and the weight gain attributable to the layer formation was noticed. Layer thicknesses were then evaluated on polished cross sections observed by electronic microscopy (figure 2) and coating densities have been calculated. All these values are reported in the table 1.

TABLE 1. Several values of sols and coatings.

Sol reference	$\%_v$ of alcohol	[precursors]	Weight gain	Thickness	Density
A	60%	1.1mol/L	1.1g/m²	1.0µm	1.1
B	3%	2.0mol/L	5.0g/m²	3.0µm	1.7
C	0%	0.6mol/L	0.7g/m²	0.8µm	0.9

Relative to the coating densities, an increase of the network compactness is clearly shown: for the sol A, that is attributed to the addition of MAP because the methacrylate functions can crosslink the inorganic network (20). In the same way, GPTMS, in the sol B, contains an epoxy ring bonded to the organic chain. This ring can be opened during the thermal treatment (14) and can induce an increase of the network reticulation.

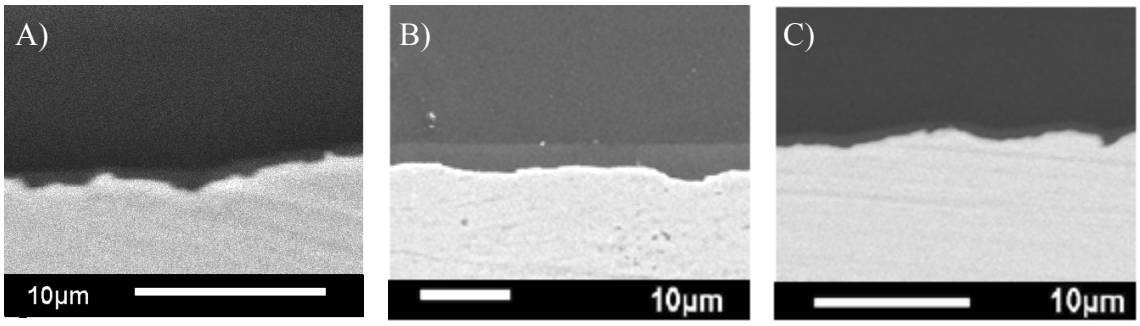

Figure 2. Cross-sections of a) coating A, b) coating B and c) coating C observed by electronic microscopy.

Micrographs of cross sections highlight the very good leveling of sol-gel layers on the substrate for each coated samples. Coatings are conformal and homogenous, and a good adhesion has been reported by industrial tests (ISO 2409 and 6272).

Durability of coatings under corrosive media

To evaluate corrosion protection efficiency, several analyses were investigated. Firstly, a typical industrial accelerated corrosion test has been carried out to highlight white rust formation under alternation of wet and dry atmospheres. This test is frequently used to predict corrosion resistance in real exposure conditions. Secondly, electrochemical analyses as polarization curves and EIS measurements have been performed to underline protection mechanisms of the systems immersed in an electrolyte.

Accelerated corrosion test. Three coated samples for each system (A, B, C) were placed in the exposure chamber. For all systems, the average weight gain due to the white rust formation was recorded after each cycle. Plots of sample weight gains, compiled in the figure 3, underline the strong reduction of the oxidation for all coated samples in comparison of the uncoated zinc. Before the fourth cycle, no oxidation is noted for coated samples. Besides, after the seventh cycle, plots show a slight increase of the weight gain.

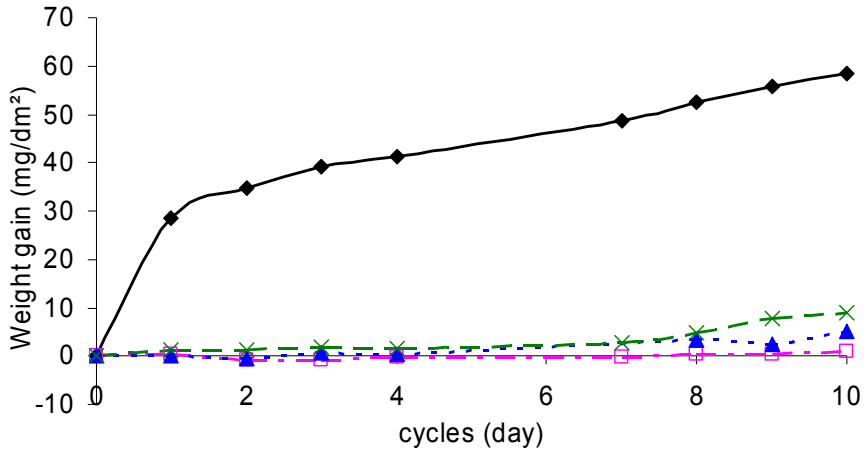

Figure 3. Weight gain of uncoated zinc (◆), coating A (□), coating B (▲) and coating C (■) during 10 cycles.

But, looking at sample photographs (figure 4.) after four and ten cycles, it can be noted that no rust is present on the surface for A & B coated samples. The slight increase of the weight gain can just be attributed to the white rust forming on edges. This oxidation is due to an accumulation of sol before the drying step, which induces layer brittleness on edges (21). However, for coatings C, general corrosion is observed from the fourth cycle, but the weight gain cannot be seen because it remains under the error bar (around 1mg/dm²).

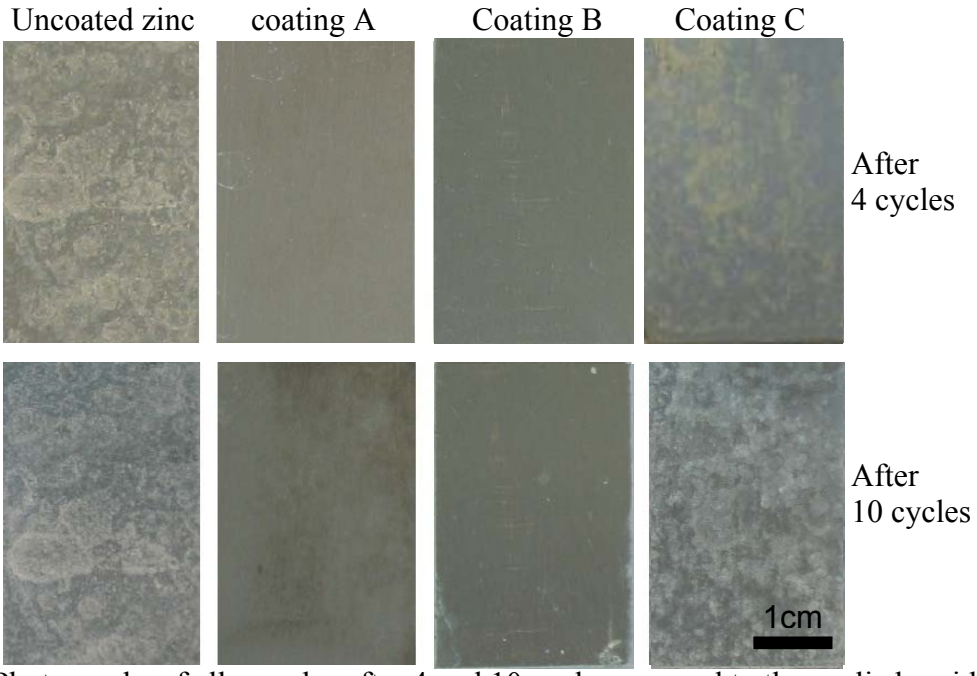

Figure 4. Photographs of all samples after 4 and 10 cycles exposed to the cyclic humidity test.

Electrochemical analyses. In order to determine the global electrochemical behavior of the system "layer + substrate", polarization curves have been plotted (figure 5.). It can be noted on these graphs, a shift of the open circuit potential for all coated samples that is correlated to an increase of the metal nobility; surface reactivity has decreased. Furthermore, anodic parts highlight a reduction of the current density at higher potentials that means a similar decrease of the oxidation reaction kinetics.

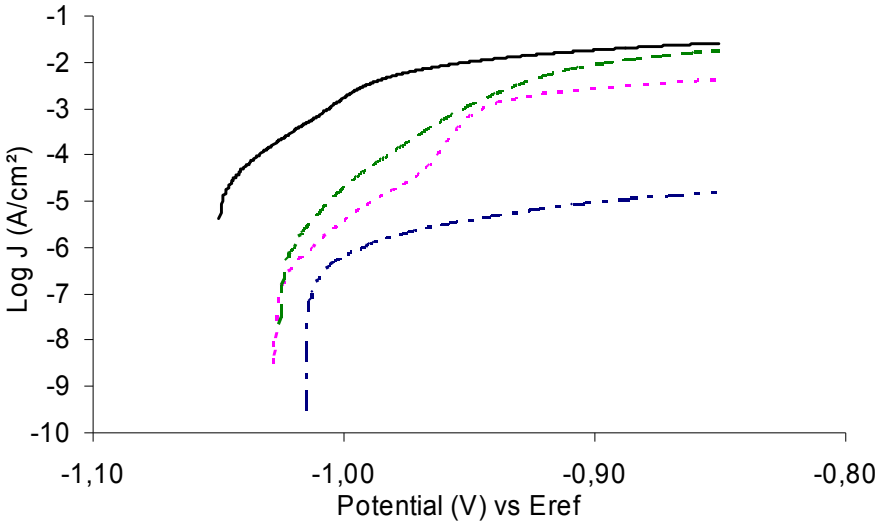

Figure 5. Polarization curves of uncoated zinc (—), coating A (- - -), coating B (- – -) and coating C (– –) after 1h of immersion in NaCl 0.5mol/L.

This decrease is linked to the barrier effect of the sol-gel coating, which is a physical barrier to the ionic migration of the electrolyte ions to the metal surface. Indeed, there is a

higher reduction of the current density (around three orders of magnitude) for B coated samples that could be attributed to a thicker and denser layer.

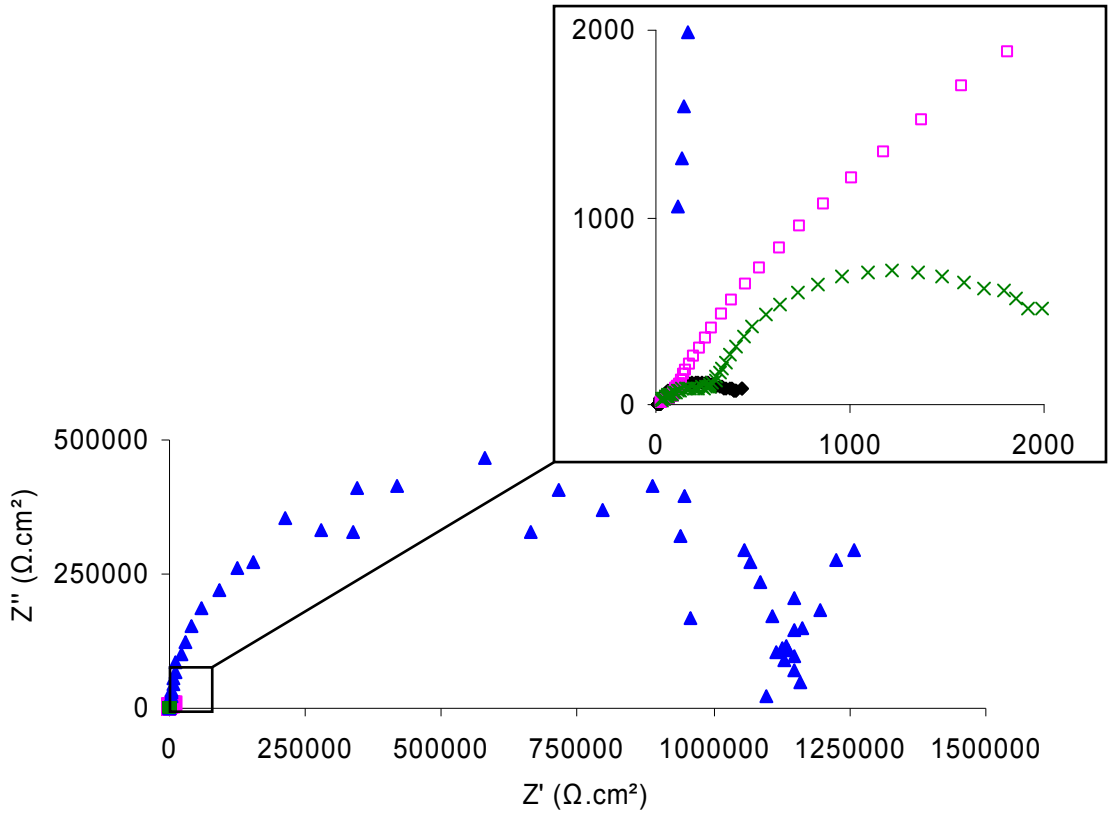

Figure 6. Nyquist representation of uncoated zinc (◆), coating A (□), coating B (▲) and coating C (×) after 1h of immersion in Na_2SO_4 0.5mol/L.

In addition, for EIS measurements, Nyquist representation underlines the very high resistance supplied by the coating B, with one well defined capacitive loop and a resistance around 1.1×10^6 Ω.cm^2. For coatings A and C lower polarization resistances are recorded, but around 5 times over than for uncoated zinc resistance (2000-2500Ω.cm^2).

On Bode representation, the high resistance of coating B is underlined by an impedance modulus at low frequencies around 10^6Ω.cm^2. For coating A, a slight improvement of the impedance modulus is observed and no significant influence is noted for coating C.

Studying the phase angle at high frequencies, similar explanations can be done: for coating C a phase angle of around 90° means a pure capacitance behavior which is a typical signature of the barrier effect (22-25). On the contrary, the light increase of the phase angle for coatings A and C show the poor barrier effect of these layers. However, for coating A, this weak capacitive behavior detected at high frequencies is balanced by a light capacitive behavior noticed at low frequencies. Therefore, electrolyte can easily enter the coating, but oxidation reaction is yet decreased. In conclusion, coating A does not really protect zinc as a physical barrier, but it contributes to slow down zinc corrosion.

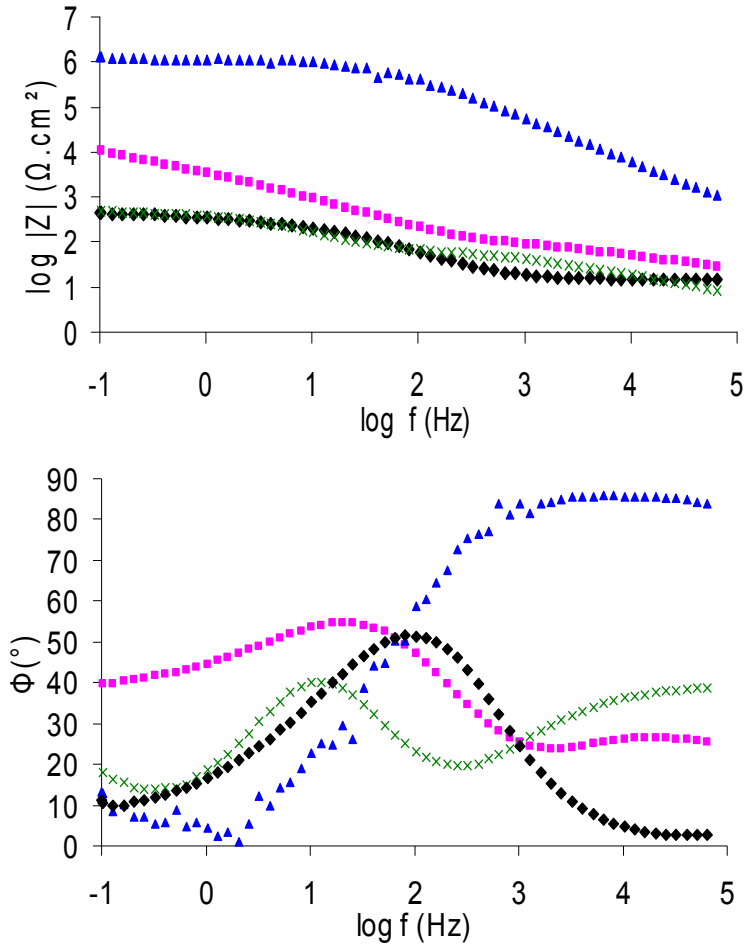

Figure 7. Bode representation of uncoated zinc (◆), coating A (■), coating B (▲) and coating C (×) after 1h of immersion in Na_2SO_4 0.5mol/L.

Corrosion test and electrochemical analyses highlight the protection efficiency of coatings A and B. However, in this paper, the environmentally friendliness is an important issue, and as shown before, and alcohol content in the sol A is too high with around 60%$_{vol.}$. So, it has been chosen to focus on protection by coating B. Nevertheless, coating B acts as a physical barrier, and the thickness can be a key parameter of its good protection. Similarly, for coating C, poor protective efficiency can be attributed to the low thickness.

So, in order to compare coating B and C avoiding the thickness influence, shaping process has been modified to obtain similar thicknesses in both cases. Concerning coating B, sol concentration was reduced and for coating C, multilayers were carried out with 15min at 80°C of drying between every dip-coating to increase the thickness.

To evaluate coating thicknesses, polished cross-sections were observed by electronic microscopy. Thicknesses were measured and reported in the table 2. Similar thickness was performed with a sol concentrated at 75% for coating B and for a multilayer for coating C with around 1.5µm. All coatings were conformal and provided good leveling of the surface.

TABLE 2. Several values of sols and coatings.

Sol reference	Sol concentration	Number of dip-coatings	Thickness
B	B_0	1	3.0µm
B	$0.875B_0$	1	2.3µm
B	$0.750B_0$	1	1.5µm
C	C_0	1	0.8µm
C	C_0	2	1.2µm
C	C_0	3	1.5µm

The protection efficiency has been investigated by EIS measurements, and Bode representations of initial and 1.5µm coatings were plotted for both B and C coatings in the figure 8.

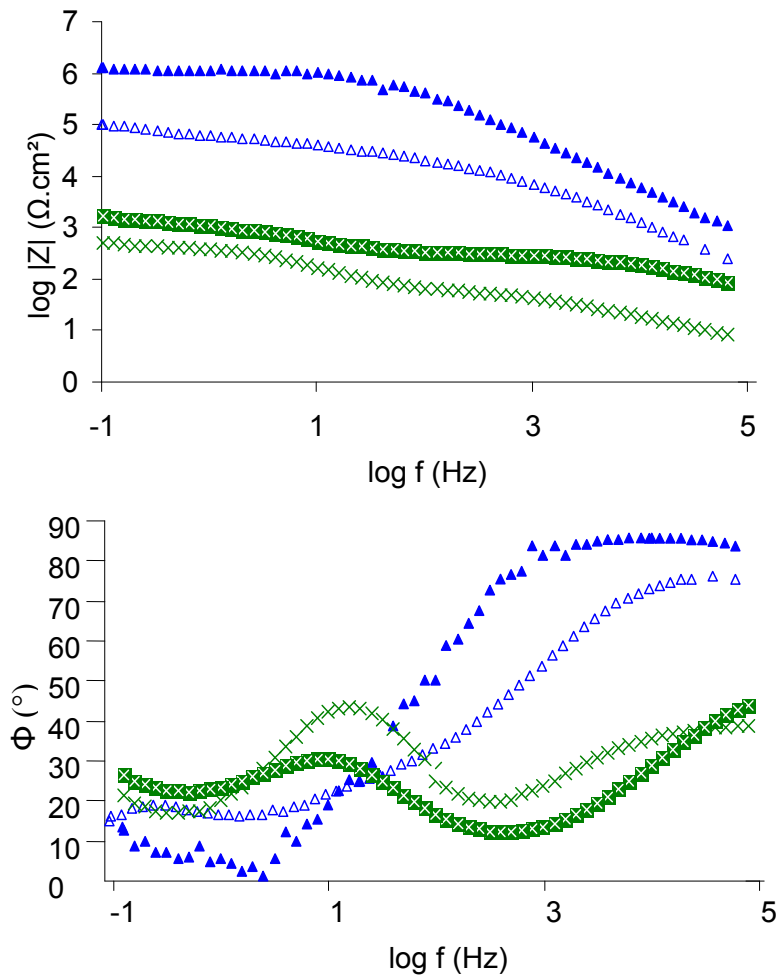

Figure 8. Bode representation of coating B 3µm thick (▲), coating B 1.5µm thick (Δ), coating C 0.8µm thick (×) and coating C 1.5µm thick (⊠)

It can be seen that concerning coating C, the increase of thickness leads to a slight improvement of the impedance modulus (nearby one order of magnitude) and a slight

decrease of the phase angle at high and medium frequencies. Protective efficiency of coating C is not clearly enhanced.

Furthermore, thickness decrease of coating B contributes to a reduction of the impedance modulus. In addition, a shift of the time constant to higher frequencies and lower phase angle is shown. That is due to the reduction of the physical barrier effect.

This experiment underlines that, protection properties for coating B remains higher than for coating C at similar thicknesses, particularly for the barrier effect that is clearly better. So, coating B efficiency is not only due to the high thickness, but also to the high compactness that reduces the electrolyte insertion in the network.

Behavior under immersion in Na_2SO_4 0.5mol/L. As shown before, with the accelerated corrosion test, two coatings provide promising anticorrosive properties; coatings A and B. But electrochemical responses are very different. In order to study and compare the behavior of these coatings, samples were maintained into Na_2SO_4 0.5mol/L solution during one week and EIS measurements have been carried out after 1h, 4h, 24h and one week. All Bode representations are compiled in figures 9.a and 9.b.

For coating A behavior during immersion, it can be noted that all Bode representations are similar whatever the immersion time, except at low frequencies. Under 10Hz, a drop in phase angle can be observed during the immersion, from 40° to 20°. This is probably due to a lost of oxidation reduction ability probably correlated to the inhibitor consumption.

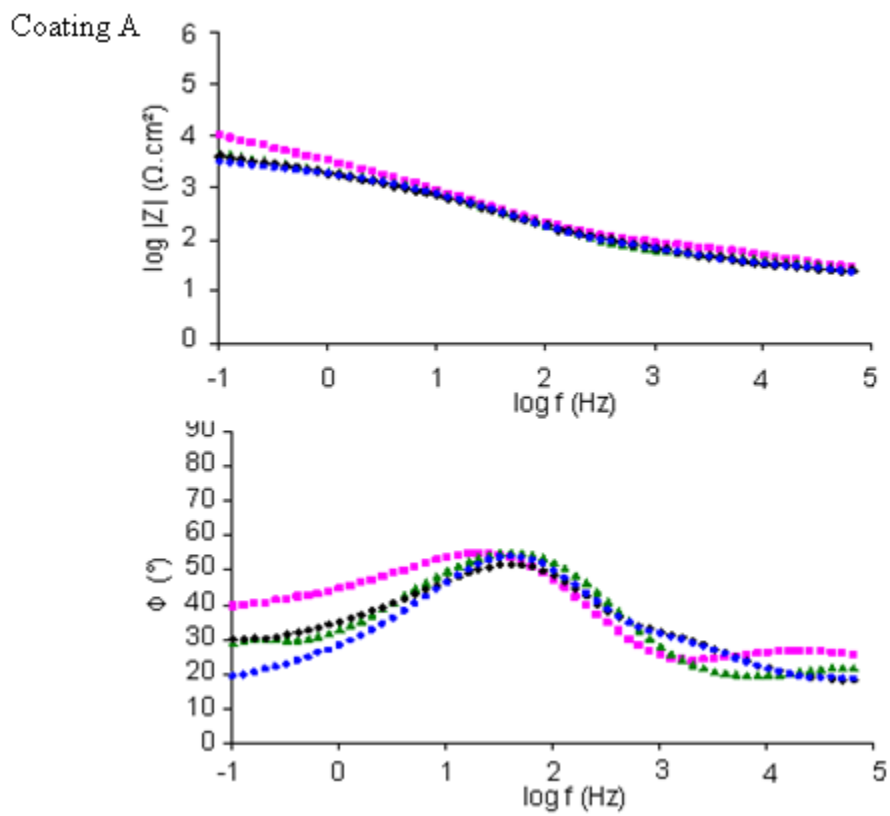

Figure 9.a Bode representation of coatings A after 1h (■), 4h (▲), 24h (◆) and one week (●).

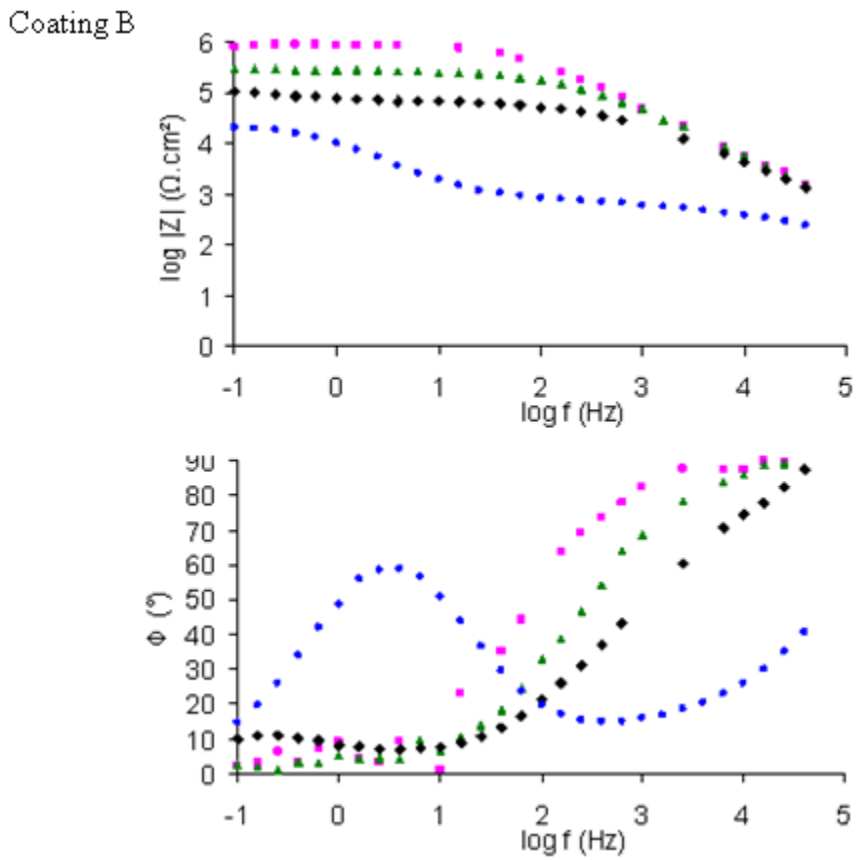

Figure 9.b Bode representation of coatings B after 1h (■), 4h (▲), 24h (◆) and one week (●).

Regarding coating B, plots show that the immersion in the electrolyte damages the barrier effect of the layer. In fact, a shift of the time constant is simultaneously observed with a significant drop in impedance modulus of one order of magnitude during the first day of immersion due to the electrolyte insertion in the coating. In addition, we can say that after one week, the barrier effect disappears and a second time constant linked to the corrosion products arises. After this, no more protection is offered by coating B.

Conclusions

By sol-gel route, three different precursor families have been studied to replace chromate based treatments for zinc protection against corrosion. Two of them have exhibited good protective properties: coating A and B; one performed from an alcoholic solution (coating A) and a second one with only 3%$_v$ of alcohol contained in the sol (coating B).

Both systems have shown very good protection in accelerated corrosion test: no white rust was observed on samples after ten cycles in cyclic humidity test. In addition, polarization curves underline an increase of nobility for A and B coated zinc samples, with a reduction of current densities and oxidation kinetics.

Moreover, EIS analyses have highlighted the high barrier effect of coating B with a strong capacitive effect at high frequencies. Whereas low barrier effect was found for coating A, a light capacitive behavior has been noticed at low frequencies. EIS

measurements after immersion in the electrolyte revealed a very slow reduction of coating A resistance probably due to the inhibitor consumption. On the other side, for coating B, a defect in barrier properties is clearly shown due to the electrolyte penetration in the coating during long immersion.

In conclusion, protection against corrosion has been reached by an environmentally friendly process (no toxic compounds and low VOC content). Furthermore, long term immersion of coated samples has underlined a significant degradation in protection efficiency. Future prospects will be turned to the addition of inhibitor effect to the coating B, perhaps by introducing encapsulated inhibitor agent.

References

1. D. de la Fuente, J.G. Castaño, M. Morcillo, Corrosion Science 49 (2007) 1420-1436.
2. E.E. Foad El Sherbini, S.S. Abd El Rehim, Corrosion Science 42 (2000) 785-798.
3. M.L. Zheludkevich, R. Serra, M.F. Montemor, I.M.M. Salvado, M.G.S. Ferreira, Surface and Coatings Technology 200 (2006) 3084-3094.
4. C.J. Brinker and G.W. Scherer, Sol-gel Science, 1990.
5. D. Wang, G.P. Bierwagen, Progress in Organic Coatings 64 (2009) 327-338.
6. T.P. Chou, C. Chandrasekaran, S.J. Limmer, S. Seraji, Y. Wu, M.J. Forbess, C. Nguyen, G.Z. Cao, Journal of Non-Crystalline Solids 290 (2001) 153-162.
7. J. Liu, J.C. Berg, J. Mater. Chem. 17 (2007) 4430.
8. A.S. Hamdy, D.P. Butt, Surface and Coatings Technology 201 (2006) 401-407.
9. Y.-S. Li, A. Ba, M.S. Mahmood, Electrochimica Acta 53 (2008) 7859-7862.
10. R.L. Parkhill, E.T. Knobbe, M.S. Donley, Progress in Organic Coatings 41 (2001) 261-265.
11. S.S. Pathak, A.S. Khanna, Progress in Organic Coatings 62 (2008) 409-416.
12. A. Cousture, P. Lenormand, S. Manov, F. Ansart, Proceeding of “Matériaux 2006”, Dijon, France (2006).
13. V. Meiffren, F. Ansart, P. Lenormand, S. Manov, proceeding of “Eurocorr 2009” (SS 05-P-7919).
14. V. Meiffren, K. Dumont, P. Lenormand, F. Ansart, S. Manov, Progress in Organic Coatings (2011) doi:10.1016/j.porgcoat.2011.03.025.
15. A.L.K. Tan, A.M. Soutar, Thin Solid Films 516 (2008) 5706-5709.
16. S.V. Lamaka, M.F. Montemor, A.F. Galio, M.L. Zheludkevich, C. Trindade, L.F. Dick, M.G.S. Ferreira, Electrochimica Acta 53 (2008) 4773-4783.
17. Y. Joshua Du, M. Damron, G. Tang, H. Zheng, C.-J. Chu, J.H. Osborne, Progress in Organic Coatings 41 (2001) 226-232.
18. M.F. Montemor, A.M. Simões, M.G.S. Ferreira, Progress in Organic Coatings 44 (2002) 111-120.
19. K. Aramaki, Corrosion Science 43 (2001) 2201-2215.
20. S.V. Asmussen, S.L. Giudicessi, R. Erra-Balsells, C.I. Vallo, European Polymer Journal 46 (2010) 1815-1823.
21. C.J. Brinker, G.C. Frye, A.J. Hurd, C.S. Ashley, Thin Solid Films 201 (1991) 97-108.
22. X. Zhong, Q. Li, J. Hu, S. Zhang, B. Chen, S. Xu, F. Luo, Electrochimica Acta 55 (2010) 2424-2429.

23. M. Garcia-Heras, A. Jimenez-Morales, B. Casal, J.C. Galvan, S. Radzki, M.A. Villegas, Journal of Alloys and Compounds 380 (2004) 219-224.
24. S.S. Pathak, A.S. Khanna, Progress in Organic Coatings 62 (2008) 409-416.
25. A.M. Cabral, W. Trabelsi, R. Serra, M.F. Montemor, M.L. Zheludkevich, M.G.S. Ferreira, Corrosion Science 48 (2006) 3740-3758.